EVALUATION OF MICROSTRUCTURE, MECHANICAL AND TRIBOLOGICAL PROPERTIES OF AA6061 REINFORCED WITH SIC AND CUO PARTICLES BY FRICTION STIR PROCESSING

S. Vijayakumar[1*], M. Naga Swapna Sri[2], P. Anusha[2], D. Gupta[3,4], E. Scutelnicu[5]

[1]Department of Mechanical Engineering, Saveetha School of Engineering, SIMATS, Saveetha University, Tamil Nadu, India
[2] Department of Mechanical Engineering, Prasad V. Potluri Siddhartha Institute of Technology, Vijayawada, India
[3]Department of Mechanical Engineering, Graphic Era Hill University, Uttarakhand, India
[4]Department of Mechanical Engineering, Graphic Era Deemed to be University, Uttarakhand, India
[5]Centre for Advanced Research in Welding, "Dunarea de Jos" University of Galati, Galati, Romania
*Corresponding author's e-mail address: vijaysundarbe@gmail.com

ABSTRACT

Friction Stir Processing (FSP) is a great solid-state surface modification method that can be employed to enhance the mechanical and tribological properties of metallic materials by using reinforcement particles. In the present study, AA6061 aluminium alloy plates with 6mm thickness were subjected to FSP process with constant parameters of 1000 rpm rotational speed and 50 mm/min traverse speed, by employing a cylindrical taper pin tool. Silicon carbide (SiC) and copper oxide (CuO) particles were incorporated in various quantities (1 to 4 wt %) to achieve surface metal matrix composites and to evaluate the impact of the reinforcement on the AA6061 alloy mechanical and wear properties. The microstructure investigation, made by optical microscopy method, demonstrated a significant change in grain structure and a uniform distribution of particles in the stir zone. Among four composites samples, the specimen reinforced with 1 wt % SiC and 3 wt % CuO (sample 3) exhibited excellent properties such as tensile strength of 190.7 MPa, elongation of 8.2%, hardness of 72.9 HV, and wear rate of 0.0526 mm³/Nm. The fracture surface analysis, performed by Scanning Electron Microscopy (SEM) technique, revealed reduced number of dimples and absence of visible cracks, as well as improved resistance to fracture and adequate structural integrity. Furthermore, the analysis of the worn surface indicated shallow grooves and minimal debris, confirming diminished abrasive wear. The results achieved by the methods presented above make the optimized FSP-treated AA6061 composite a promising material for industrial applications such as automotive components, aerospace structures, and tooling elements.

KEYWORDS: Friction Stir Processing, AA6061 alloy, silicon carbide, copper oxide, mechanical properties, microstructure, hardness, wear

1. INTRODUCTION

Friction Stir Processing (FSP) is a proficient solid-state method that is frequently applied to improve the properties of aluminium alloys through localised microstructure modification process. This process is possible by employing a rotating tool that generates by friction a great amount of heat at interface between the tool and metal surface, resulting significant plastic deformation and dynamic recrystallisation in the affected area, hence improving the grain structure and ensuring uniform phase distribution. Multiple investigations have validated the effectiveness of the FSP process in modifying the surface properties of diverse grades of aluminium alloys, determining significant improvement of materials mechanical properties, such as enhanced hardness and improved resistance to corrosion [1-2]. Extensive studies have shown that ceramic particles [3-5], such as boron carbide (B_4C), titanium carbide (TiC), boron nitride (BN), vanadium carbide (VC), silicon carbide (SiC), and copper oxide (CuO), can be effectively incorporated into aluminium alloys through the FSP procedure. The particles reinforcements have a similar

Date of submission/acceptance: 15.08.2025/15.12.2025
https://doi.org/10.35219/awet.2025.06

role as the grain refiners, promoting a finer grain structure, increasing the strength and stiffness while the wear resistance is improved by inhibiting the dislocation movement and facilitating the dynamic recrystallisation within the stir zone.

Besides, the selection of reinforcement particles and the process parameters have a significant and substantial influence on the properties and quality of the surface processed by FSP. The tool rotational speed has been recognised as a critical factor that has a major influence on the distribution of reinforcement particles within the treated zone [6-9]. An increase in rotational speed of the tool typically results in higher heat input and enhanced plastic flow, facilitating better dispersion of particles and development of finer structure of grains. An increase in traverse speed can boost the grains refining due to more reduced temperature exposure that determines the decrease of grains development time. However, the optimal properties and structure performance relies on maintaining these characteristics within defined boundaries. Anyhow, both excessively high and low values may adversely affect the material flow, induce tool wear, or result in defects such as tunnel voids and non-uniform mixing [6-9].

A wide range of studies has investigated various reinforcements used to enhance the mechanical and tribological properties of aluminium alloys by FSP method. D. Divekar et al. [10] employed the Bobbin Tool Friction Stir Processing (BT-FSP) technique to incorporate B_4C particles into 6 mm thick Al-Mg-Si alloy plates. The analysis revealed that the BT-FSP processed composites exhibited considerable aggregation of B_4C particles and cracks formation in certain areas. The deficiencies were developed mostly from the insufficient forging operation, leading, further, to the buildup of reinforcing particles within the cracks. Despite these limitations, the microhardness analysis demonstrated a significant increase in the surface hardness of the BT-FSP specimens compared to the base material. The findings underscore the crucial role of the tool geometry and of process parameters optimisation in achieving uniform distribution of reinforcement particles and flawless composite on aluminium surface processed by FSP technique.

M. R. Kumar [11] investigated the influence of the pinless friction stir tool in FSP of AA6061 alloys. Increasing the tool rotational speed to 1200 rpm, while keeping a traverse speed of 25 mm/min, the corrosion resistance, mechanical characteristics, and surface microstructure were significantly affected. The microstructure examination revealed a significant increase in the microhardness of the treated samples, accompanied by a significant decrease in grain size. In another studies, Rice husk ash (RHA) was used as reinforcement material to develop composites on the surface of AA6061 aluminium alloy through FSP. The research focused on assessing the particles dispersion and microhardness of the treated specimens. The results demonstrated that the AA6061 alloy, reinforced with 5 wt % RHA and processed with rotational speed of 1200 rpm, showed the most uniform particle distribution and the greatest average microhardness value (80 HV) [12].

Ch. M. Rao et. al. [13] employed TiB_2/Al_2O_3 particles to assess the microhardness, tensile strength, and microstructure of AA6061/TiB_2/Al_2O_3 alloy surface composites. This work inspected the impact of tool design and process factors on microstructural variations and effectiveness of the modified surface layer, providing important insight into the behaviour and potential applications of advanced composite materials.

M. R. Chanamallu et al. [14] investigated the fabrication of AA6061/SiC/Al_2O_3 composites and analysed the influence of various process parameters on the mechanical properties. Among the samples, the sample S3 showed the highest tensile strength (185MPa). The optimal conditions for achieving maximum tensile strength were found to be the combination of rotational speed of 900 rpm, and traverse speed of 15 mm/min. Ouyang et al. [15] investigated the thermal distribution and microstructure changes of Al alloy and copper. The researchers reported that the low strength of joints was caused by the presence of brittle intermetallic compounds developed in the nugget zone.

Shahraki et al. [16] studied the use of FSP method to fabricate AA5083 composites reinforced with ZrO_2 particles. Based on optical microscopy and SEM methods, the authors made the microstructure characterization, focusing on the shape and distribution of ZrO_2 particles within the AA5083 matrix. The findings demonstrated that the incorporation of ZrO_2 particles significantly enhanced the hardness and wear resistance of the composite, comparing to the unreinforced AA5083, the advantageous effect of ZrO_2 reinforcement on the mechanical properties of AA5083 composites being obvious.

B. R. El-Eraki et al. [17] investigated the application of hybrid Al_2O_3 and graphite particles in AA6061 to fabricate a surface composite by multiple-pass FSP. The results demonstrated that the composites enhanced with alumina particles attained a peak ultimate tensile strength of 213 MPa. The increase in hardness in the stir zone of samples processed by FSP was significantly greater after post-heat treatment, but the number of passes had minimal effect on the hardness profile.

M. R. Ch et al. [18] studied the TiB_2 reinforcement with three distinct slot thicknesses from 1 to 2 mm, used to achieve surface composites on Al6061-T6 alloy. The tribological properties were evaluated at two distinct sliding velocities: 0.314 m/s and 0.48 m/s. At reduced loads, it was found an inconsequential variation in the wear rate of surface composites carried out with varying slot dimensions.

K. N. Uday [19] studied the Al6061 alloy reinforced with B4C and Cr2O3 separately to obtain

Al6061 + B4C and Al6061 + Cr2O3 aluminium metal matrix composites (Al MMC). Al composites were produced by stir casting with weight percentages of 2%, 4%, and 6%. The incorporation of Al MMC was essential for developing appropriate components. The authors reported that increasing the travel speed from 20 to 25 mm/min, an increase up to about 59% of tensile strength was observed. Besides, the predictive average accuracy of response surface methodology (RSM) and the artificial neural network (ANN) were found 98.26 and 94.86, respectively.

Mohammed Yunus and Rami Alfattani are produced AA6061 via a dual stir casting technique, incorporating variable volume fractions of B4C (5-15%) and Gr (110-20%). It was observed that reinforcement with Al alloy is equally distributed inside the primary matrix, creating a mechanically mixed layer characterised by interfacial reactions. This layer decreases wear loss and COF, particularly with increased quantities of B4C and Gr, as they exhibit minimal aggregation of the reinforced material. Micro-hardness investigations reveal that the hardness of HMMC escalates with an increase in the volume fraction of reinforced particles and the sliding distance and the compression test demonstrated a 22% enhancement compared to AA6061 [44]. In another study,

S. Kaliappan et.al. [45] analysed the mechanical characteristics for Al 6061-SiC-AlN composures the result found that the incorporation of SiC and AlN reinforcements enhanced the UTS from 328 to 385 MPa, hardness from 302 to 724 HN and the compressive strength from 145 to 178 MPa.

Based on the literature reviews [11], [15], [19], [44-45], Al 6061 reinforced with different reinforcements (Rice husk ash, B4C, hybrid Al_2O_3/graphite particles, Cr2O3, Gr and SiC-AlN). It was found that no studies have explored and reported results on 6061 aluminium alloy reinforced with CuO/SiC particles in different mixtures by applying the Friction Stir Processing (FSP) procedure.

To fill this research gap and to improve the scientific knowledge in this area, four distinct combinations of SiC and CuO powder mixtures like 1 wt % SiC + 1 wt % CuO, 1 wt % SiC + 2 wt % CuO, 1 wt % SiC + 3 wt % CuO, and 1 wt % SiC + 4 wt % CuO have been investigated. The analysis of the microstructure characteristics, mechanical behaviour and wear properties of FSP AA6061 joints provides novel insights into the synergistic effects of CuO and SiC reinforcements used to enhance the performance of the Al6061 alloy.

2. MATERIALS AND METHODS

2.1. Materials

AA6061 sheets with dimensions of 200 x 50 x 6 mm^3 were prepared to be processed by FSP technique. The chemical composition of the AA6061 is presented in table 1 [20-21]. This material was chosen due to its excellent mechanical properties, high corrosion resistance, and wide applicability in structural and automotive components.

Before surface processing, several circular micro-holes with diameter of 2 mm and depth of 1.9 mm were precisely drilled into the surface of the AA6061 plate. These cavities were uniformly distributed with 2.5 mm spacing and packed with homogenous mixture of CuO and SiC powders.

Table 2 shows the thermo-physical properties of CuO [22-24] and SiC particles [25]. The reinforcement powders, having average particle size of 10 µm, were carefully filled into the pre-drilled holes to ensure uniform dispersion during the stirring phase. Four combinations of SiC and CuO powders, as seen in table 3, were mixed and used to perform 4 samples whose microstructure, mechanical properties, and wear resistance were, subsequently, examined, analysed and discussed in detail.

2.1.1. Process and Parameters

The welding process was performed with the FSP equipment (Fig. 1) that had a taper cylindrical pin tool. Figures 2a and 2b illustrate the Al6061 alloy plates before and during the FSP procedure, respectively. Figure 2c shows the taper cylindrical tool with shoulder diameter of 20mm and a pin length of 2mm and pin diameter of 6mm for this work.

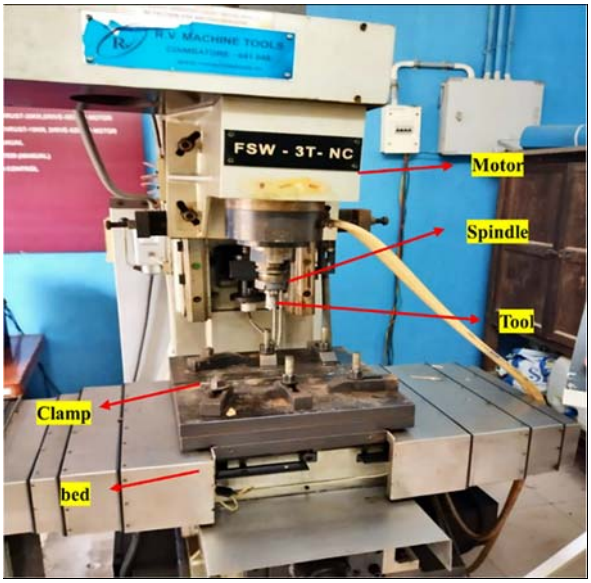

Fig. 1. Friction Stir Processing (FSP) equipment

To ensure a constant heat input and an adequate material flow [26], the whole FSP process was performed with constant tool rotational speed of 1000 rpm and traverse speed of 50 mm/min for all four samples illustrated in figure 2d. The main FSP process parameters applied to carry out four samples with four combinations of SiC and CuO particles (particle size: 50 nm) are centralised in table 3.

2.1.2. Tensile Testing

The AA6061 specimens for tensile testing were precisely machined by wire-cut electrical discharge machining (EDM) technique. The specimens were cut perpendicular to the stir zone in order to accurately assess the mechanical behaviour across the processed region. All samples were prepared according to the ASTM E8 standard [27], and the uniaxial tensile testing was conducted by employing a Universal Testing Machine (UTM).

Based on the experimental tests, the results regarding the tensile strength and elongation properties of the samples processed provided critical insights in terms of reinforcement effect on the mechanical performance of the Al6061 alloy reinforced with different combinations of SiC and CuO particles.

Table 1. Chemical composition of AA6061 base material [20]

Al	Mg	Fe	Si	Cu	Ti	Mn	Zn	Cr
95.85-98.56	0.8-1.2	0.0-0.7	0.4-0.8	0.15-0.40	0.0-0.25	0.0-0.15	0.0-0.25	0.04-0.35

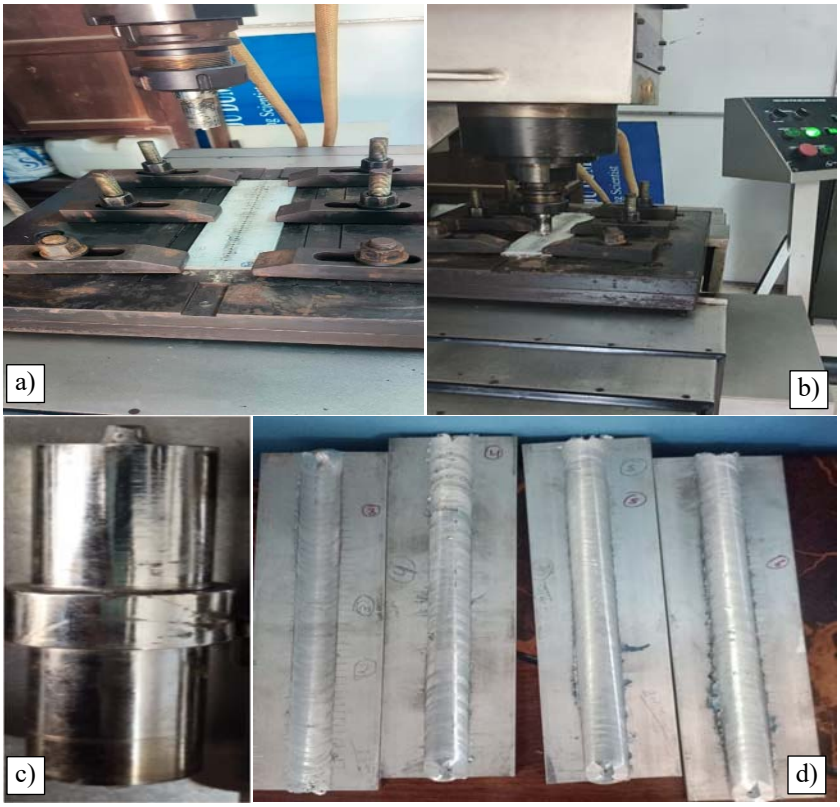

Fig. 2. FSP processing of AA6061: a) AA6061 plates before FSP process; b) AA6061 plates during FSP process; c) FSP tool; d) AA6061 samples reinforced with SiC and CuO by FSP method

Table 2. Thermo-physical properties of CuO and SiC particles

Thermo-physical properties of CuO particles		**Thermo-physical properties of SiC particles**	
Thermo-physical property	**Values**	**Thermo-physical property**	**Values**
Purity	98%	Maximum Temperature	1350 °C
Density	6550 kg/m^3	Open Porosity	< 0.2 %
Morphology	Irregular shapes	Density	3010 kg/m^3
Particle Size	42 nm	Bending Strength	230 (20 °C) MPa 270 (1200 °C) MPa
Specific heat	530.5 J/kg·K	Thermal Conductivity	42 (1200 °C) W/m·K
Bulk density	780 kg/m^3	Elastic Modulus	320 (20 °C) GPa 300 (1200 °C) GPa
SSA	22 m^2/g	Thermal Expansion coefficient	4.4 K^{-1}×10^{-6}
True Density	6450 kg/m^3	Acid and alkali resistance	Excellent
Thermal Conductivity	21 W/m·K	Mohs hardness	12

Table 3. Main FSP process parameters applied for different particles mixtures

Sample	Rotational speed, [rpm]	Traverse speed, [mm/min]	SiC, wt. [%]	CuO, wt. [%]
S1	1000	50	1	1
S2			1	2
S3			1	3
S4			1	4

2.1.3. Microstructure Analysis

To better understand the effect of particles mixture reinforcement on the fracture mechanism of the AA6061 material processed by FSP method, a microstructure analysis was made by Scanning Electron Microscopy (SEM) method, with ZEISS EVO-18 equipment. This investigation method, a highly versatile technique that provides valuable information on microstructure and fracture phenomenon, was carried out for the samples reinforced with SiC of 1wt % and CuO of 2 wt %, and for that reinforced with particles mixture of 1wt % SiC and 3 wt % CuO particles.

2.1.4. Vickers Hardness Testing

The Vickers microhardness testing was conducted on polished cross-sections of the weld nugget to evaluate the hardness profile across the friction stir processed zone with Vickers hardness equipment. The microhardness measurements were made according to the ASTM E92 standard with a constant load of 15 N that was applied for a dwell time of 15 seconds [28]. The resulting data provided significant information on the hardness gradient and material response determined by the SiC and CuO particles reinforcement and processing conditions.

2.1.5. Wear Testing

To assess the wear behaviour of the processed composites samples, a standard pin-on-disc tribometer was setup and employed. The composites specimens were tested against a rotating steel disc under controlled normal loading conditions.

To ensure consistency and reproducibility of results, all wear tests were performed according to the ASTM G99-17 standard. The wear testing specimens were machined with dimensions of 10 × 10 × 6. in [mm], and were surface-finished with 800-grit silicon carbide (SiC) paper to obtain a uniform surface roughness, compatible with that of the mating disc.

Before testing phase, each specimen was thoroughly cleaned with acetone to eliminate any surface contaminant that could influence the wear measurement. During testing phase, each of the four specimens was evaluated 15 minutes time under a constant normal load of 30 N and a rotational speed of 200 rpm.

The wear loss or wear depth was determined with a digital balance, by calculating the weight difference of the specimens before and after testing. The measured weight loss provided quantifiable information of the resistance material to wear under the specified conditions [29].

3. RESULTS AND DISCUSSION

3.1. Tensile Testing Results

The tensile testing experiments were performed for estimating the tensile strength, and elongation properties of the friction stir processed samples, the results, shown in table 4, providing critical insights into the effect of SiC/CuO reinforcement on the mechanical performance of the Al6061 alloy.

The tensile strength values and stress versus strain curve for all four samples are displayed in figure 3a and figure 3b. Based on the results presented in table 4 and figure 3, the sample 1 shows a significant enhancement in ultimate tensile strength (UTS) up to 180.1 MPa, along with an increase in elongation to 6.3%. In case of sample 2, a minor reduction to 150.6 MPa in UTS was noticed, elongation being lower (5.9%) than that of sample 1. This diminution of the mechanical properties suggests a potential limit in reinforcement effectiveness beyond which additional increments do not produce equivalent benefits. Moreover, the UTS and the elongation of the sample 4, processed with a combination of 1 wt % SiC and 4 wt % CuO particles, were recorded at 155.6 MPa and 6.8%, respectively, indicating a modest increase compared with the value reached by the sample 1.

The highest mechanical performance, meaning an optimal balance of strength and ductility, with the UTS peak of 190.7 MPa and elongation of 8.2%, was exhibited by the sample 3. This significant increase was achieved at 1000 rpm rotational speed and 50 mm/min welding speed, with reinforcement consisting of 1 wt % SiC and 3 wt % CuO particles mixture. The general trend of the enhanced UTS and elongation with the incorporation of 1 wt % SiC and 3 wt % CuO particles underscores their value as reinforcements in the aluminum matrix. These particles enhance uniform stress distribution under mechanical loading by reducing localized stress concentrations. Furthermore, the dispersion of particles may promote the microstructural refinement, limiting the grain development and microcracks propagation [30].

Figure 3b exhibits the stress-strain curve that defines the material behaviour under load, which provides precious insights into the material's strength, ductility, and failure limits. The way in which a material responds to a load depends on the material properties, in general, and to the reinforcement properties, in particular. The strain vs. stress curve confirms the conclusion drawn above in terms of the role and effect of particles mixture reinforcement on the quality of samples achieved by FSP procedure.

It can be seen that the samples 1 and 3 of AA6061 reinforced with the particles combinations consisting of 1 wt % SiC and 1% wt % CuO , respectively 1 wt % SiC and 3% wt % CuO, have a significant higher deformation capacity comparing to the samples 2 and 4. The highest mechanical performance, demonstrated by an optimal balance of strength and ductility given by the highest values of UTS and elongation, is reported for the sample 3 whose particles combination seems to be the optimal reinforcement.

Table 4. Mechanical properties and wear rate results determined by experiments

Properties	Sample			
	1	2	3	4
Tensile strength [MPa]	180.1	150.6	190.7	155.6
Elongation [%]	6.3	5.9	8.2	6.8
Hardness [HV]	70.1	69.6	72.9	75.3
Wear rate [$mm^3/N \cdot m$]	0.0785	0.0452	0.0526	0.0374

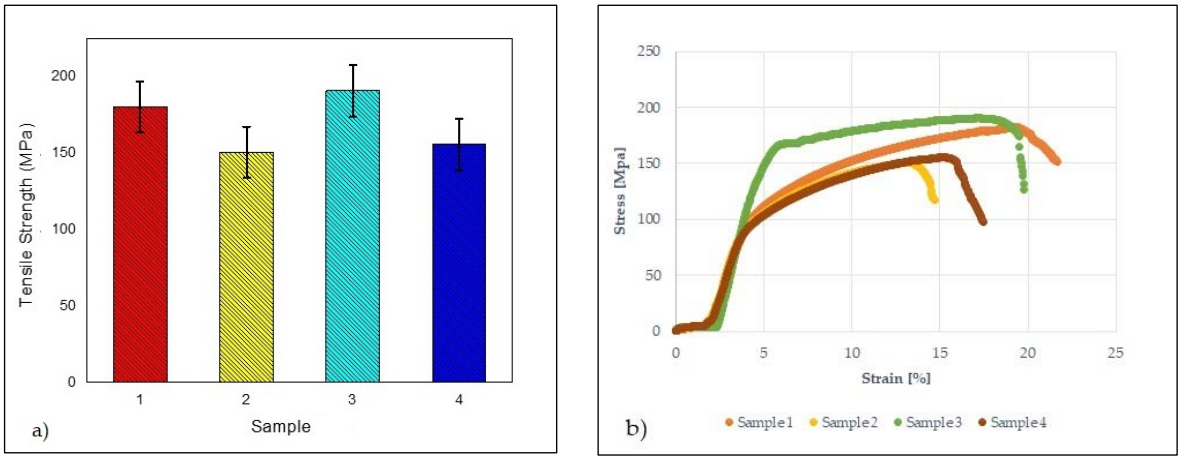

Fig. 3. Tensile testing of samples 1 to 4 reinforced with SiC and CuO particles by FSP method: a) tensile strength results; b) stress vs. strain curve

3.2. Microstructure Analysis

Figure 4 and figure 5 exhibit the SEM images, with different magnifications, of the fracture surfaces of the AA6061 alloy samples reinforced with 1 wt % of SiC and 2 wt % of CuO, as well as with 1 wt % of SiC and 3 wt % of CuO particles. The aim of this analysis was to investigate the influence of wt % of SiC and CuO on fracture behaviour of samples processed by FSP. The fracture surface of the sample 2, carried out with 1000 rpm of tool rotational speed and 50mm/min welding speed and reinforced with 1 wt % SiC and 2 wt % CuO, reveal the high depth of dimples and cavities at the left corner and centre side, as figure 4 shows. This behaviour was primarily attributed to the low reinforcement content, which may have been inadequate to refine significantly the grain structure or to establish effective load transfer mechanisms, resulting in limited plastic deformation and reduced ductility [31]. Additionally, insufficient stirring or mixing during friction stir processing combined with likely low reinforcement level caused CuO particles agglomeration, leading to development of coarse precipitates that acted as stress concentrators, especially at incoherent or semi-coherent interfaces with the aluminium matrix, and, further, to early crack initiation and propagation triggering. The non-uniform distribution, possibly caused by the suboptimal powder packing, contributed to the asymmetric localization of precipitates, particularly on the left and centre of the stir zone. Consequently, the combination of low reinforcement percentage and coarse precipitates formation reduced the toughening effect of particles, leading to a semi-brittle fracture mode characterized by the dominance of shallow dimples across the surface [32-34].

The fracture surface of the sample 3, carried out with 1000 rpm of tool rotational speed and 50mm/min welding speed and reinforced with 1 wt % SiC and 3 wt % CuO, exhibit fewer dimples with no visible cracks, indicating a more stable and uniform fracture behaviour, as it can be seen in figure 5.

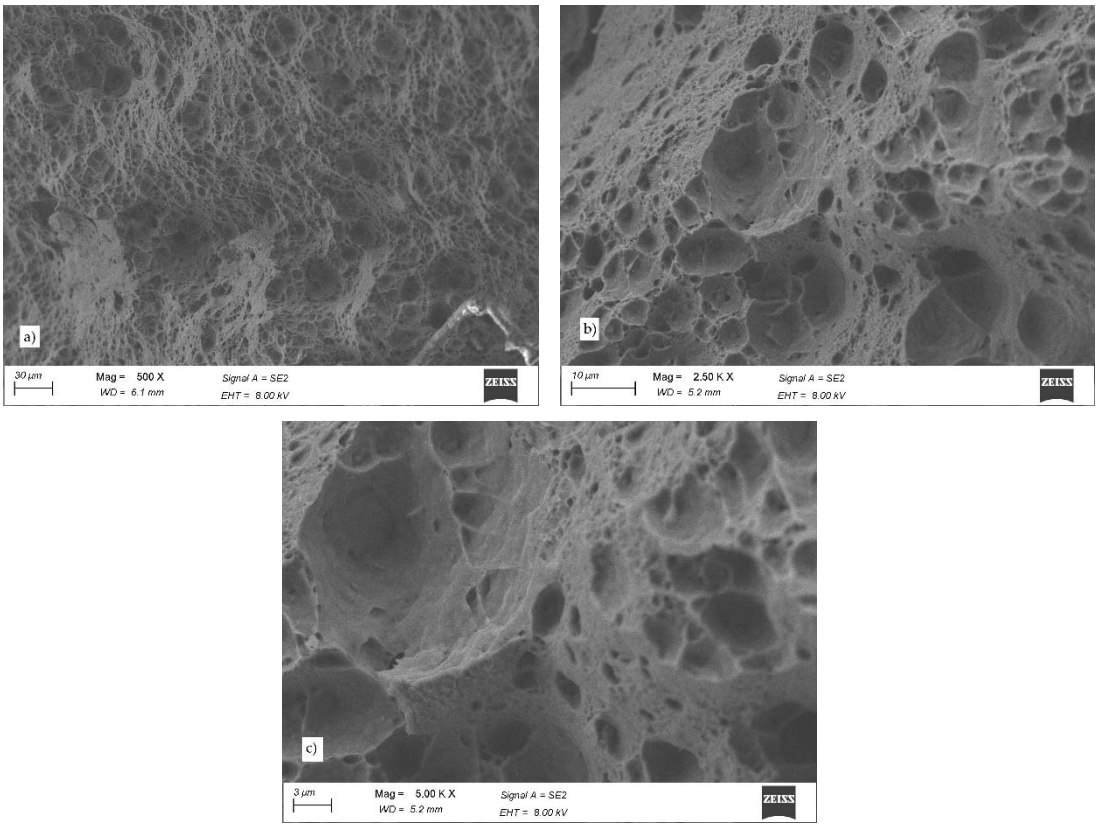

Fig. 4. SEM images of sample 2 (1000rpm, 50mm/min, 1 wt % SiC and 2 wt % CuO): a) 500 x magnification; b) 2.50 kx magnification; c) 5.00 kx magnification

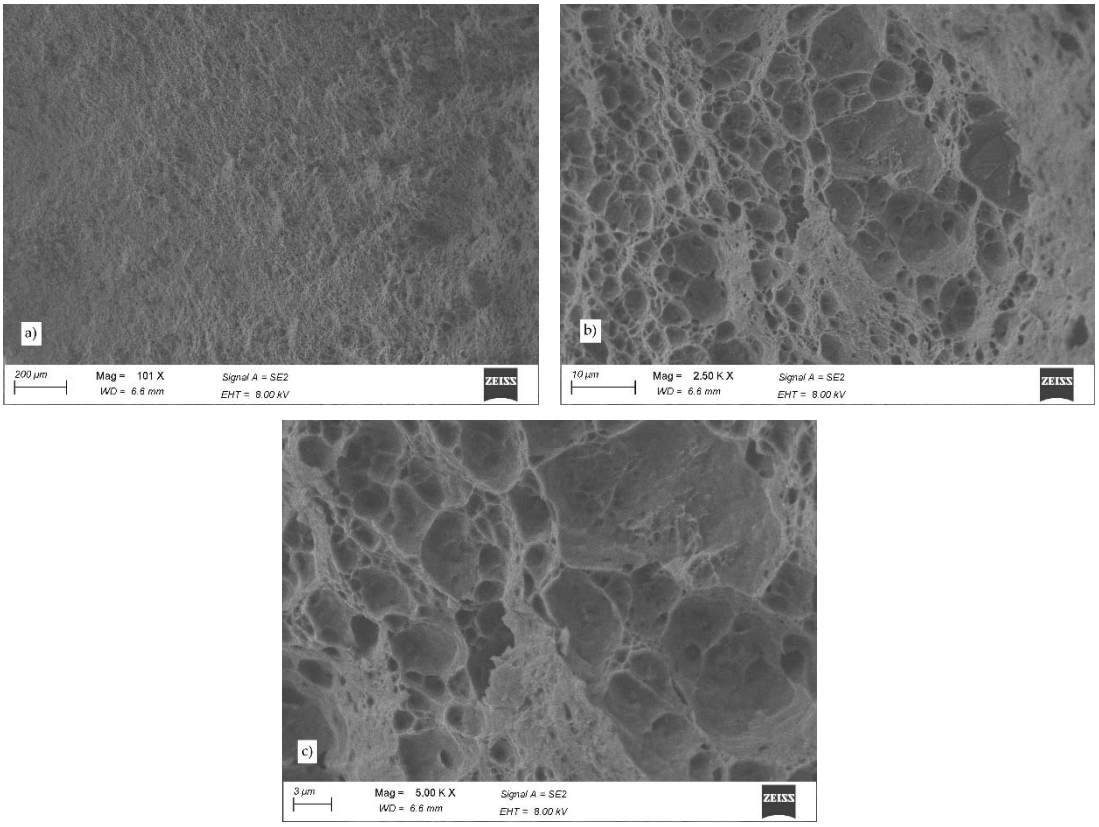

Fig. 5. SEM images of sample 3 (1000rpm, 50mm/min, 1 wt % SiC and 3 wt % CuO): a) 101 x magnification; b) 2.50 kx magnification; c) 5.00 kx magnification

Notably, the reinforcement particles, both SiC and CuO, are uniformly distributed throughout the matrix, suggesting effective mixing and appropriate dispersion during friction stir processing. This uniform distribution contributes to enhanced load-sharing capabilities and minimized stress concentrations, thereby reducing the crack initiation sites. However, despite the overall uniformity, coarse precipitates were prominently observed on the right side of the sample, possibly caused by the localized material flow or minor asymmetries in the stirring process. The reduced number of dimples suggests a transition toward a slightly less ductile fracture mode, potentially influenced by the increase of the CuO content, that may have led to localized hardening phenomenon [35, 36]. Nevertheless, the absence of cracks and the uniform particles distribution indicate improved structural integrity and fracture resistance in sample 3, comparing to sample 2.

3.3. Vickers Hardness Testing Results

Based on the results shown in table 4 and displayed in the chart from figure 6, the lowest Vickers microhardness was 69.6 HV and it was measured in the stir zone of the sample 2 which has been reinforced by FSP with 1 wt % SiC and 2 wt % CuO.

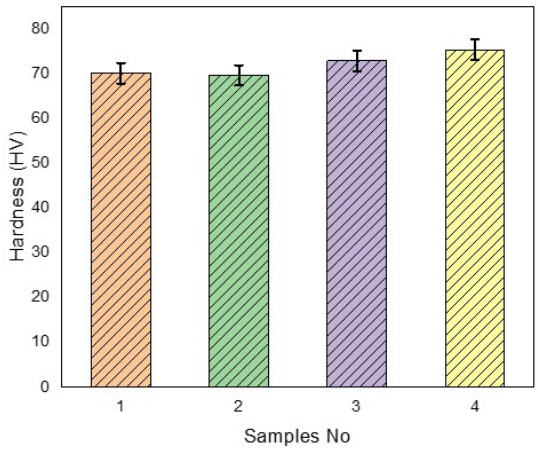

Fig. 6. Vickers hardness for samples 1 to 4 reinforced with SiC and CuO particles by FSP method

This comparatively lower hardness value can be attributed to the insufficient reinforcement concentration, which likely resulted in inadequate dispersion of particles and weak interfacial bonding between the matrix and the reinforcement particles. Additionally, the lower CuO content may not have contributed effectively to load transfer and grains boundary pinning, finally leading to limited strengthening of the matrix.

The highest hardness of 75.3 HV was measured in the stir zone of the sample 4 which has been reinforced with 1 wt % SiC and 4 wt % CuO by FSP technique, demonstrating the significant influence of larger CuO percentage on the properties of the composite material. The significant increase in hardness is primarily due to the enhanced reinforcement volume fraction, which improves the load-bearing capability and restricts the dislocation movement through the Orowan strengthening mechanism.

The higher amount of CuO, in combination with SiC particles, contributed to better dispersion, increased particle-matrix interface strength, and more effective grain refinement due to the pinning of grain boundaries during the dynamic recrystallization in the stir zone. These microstructural modifications lead to a denser and harder weld zone, thereby demonstrating the critical role of the reinforcement ratio in determining the mechanical behaviour of the hybrid composites during processing by the FSP method. When comparing the present results of the AA6061/SiC/CuO hybrid composite with other reported AA6061-based composites, the improvement in mechanical and tribological performance is evident. The resulted UTS of 190.7 MPa surpasses that of conventional single-reinforced systems such as AA6061 + Al_2O_3 ,AA6061 + SiC, and AA6061 + B_4C (175–185 MPa and TiB_2-based AA6061 composites (180–188 MPa). Similarly, the measured hardness of 75.3 Hv lies in the upper range of reported values for Al6061 composites, confirming the strengthening contribution of SiC combined with CuO.

3.4. Wear Testing Results

Based on the wear testing that was conducted by employing a pin on disc tribometer, the wear depth versus time graph clearly illustrates how a material surface is deteriorated under frictional contact over a specific period. On the Y-axis, it shows the wear depth that indicates how much material has been removed during wear testing, while the X-axis represents the testing time, in seconds (Fig. 7a). The resulting curve reflects the progression of wear, helping to understand the pattern of surface damage while the material is subjected to continuous wear [37, 38]. From figure 7, the low and the high wear depths were found for the sample 4 and sample 1, respectively. The wear rate for all samples was calculated by applying the equation (1) (see the results in table 4), where the wear rate (W) is defined by the volume difference of the material after wear (ΔV), applied normal load (L), and the sliding distance (D).

$$W = \Delta V / (L \times D) \quad (1)$$

Figure 7b shows the coefficient of friction (COF) versus time curve for each sample. The COF values vary significantly from sample to sample, ranging from the lowest value 0.18 in case of sample 1 to the highest value of 1.5 in sample 4. This variation indicates a progressive increase in frictional resistance that could be attributed to heterogeneity in material composition, surface roughness, or to the content of particles

reinforcement specific to each sample. Initially, all samples exhibit a relatively low COF, likely due to surface smoothing and material adaptation during the early stages of sliding. As time progresses, the COF has stabilized or has increased in correlation with the wear characteristics and tribological behaviour of each sample. The results suggest that, under similar testing conditions, the compositional modifications have a major influence on the frictional response.

According to the results presented in table 4, the lowest wear rate of 0.0374 mm³/N·m was observed in Al6061 alloy sample 4, reinforced with 1 wt % SiC and 4 wt % CuO. This reduced wear rate indicates enhanced wear resistance in the processed area, the phenomenon being explained by better uniform distribution of reinforcement and improved interfacial bonding between the matrix and the particles. The presence of SiC and CuO particles in optimal proportions contributes to increased surface hardness, reduced plastic deformation during sliding, and better resistance against abrasive and adhesive wear mechanisms.

The improved wear resistance observed in sample 4 can be attributed to the increased CuO percentage that may enhance the material performance through multiple mechanisms. The CuO particle is a hard ceramic that led to increasing the overall hardness of the composite, thereby improving its resistance to plastic deformation and abrasive wear. Additionally, CuO exhibits mild solid lubricating properties under sliding conditions, reducing the coefficient of friction and, consequently, minimizing the wear rate.

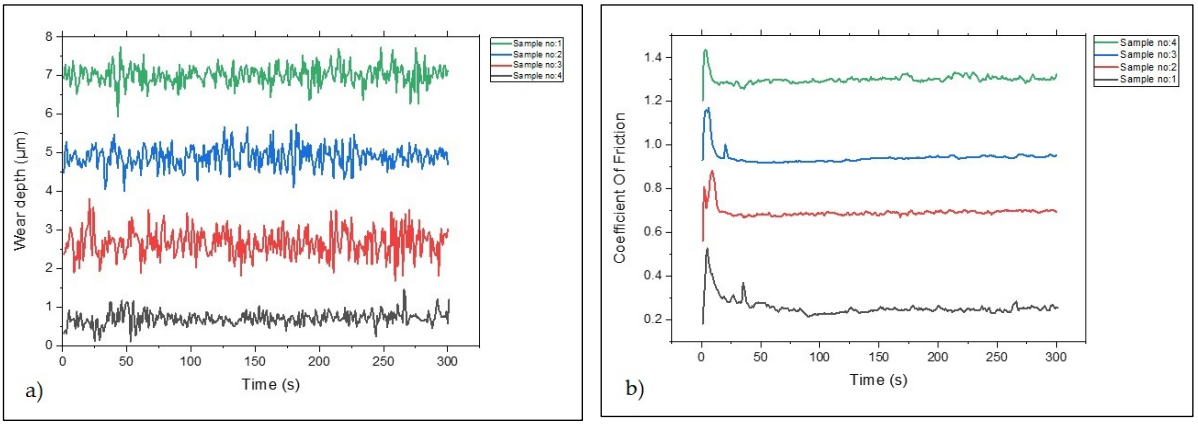

Fig. 7. Wear testing results: a) wear depth versus time; b) coefficient of friction versus time

Besides, its uniform dispersion within the matrix contributes also to microstructure refinement, resulting in better grains distribution and mechanical interlocking, and, subsequently, to development of lower localized stresses [39]. Furthermore, the CuO particles act as load-bearing reinforcements, determining a distribution of the applied load more efficiently and a more reduced stress level in the matrix. In contrast, the sample 1, which contains the least amount of CuO, does not benefit from these enhancements and, thus, the wear test exhibits higher wear depth caused by the lower hardness, higher friction, and poorer load distribution. That is why, the highest wear rate of 0.0785 mm³/N·m was found in the sample 1 that was reinforced, with 1 wt % SiC and 1 wt % CuO by FSP procedure. It is supposed that the homogeneity and the microstructure integrity of the sample may have adversely affected, leading to insufficient particle distribution and weak matrix-particle bonding. Figures 8a and 8b depict the wear morphology of the sample and sample 4, respectively. It was noticed the occurrence of track impressions and deep grooves on the surface of the Al6061 reinforced with 1 wt % SiC and 1 wt % CuO joint, that indicating a severe abrasive wear. This phenomenon could be attributed to the interaction between the hard reinforcement particles and the counterface, causing micro-cutting and plowing actions. The accumulation of substantial wear debris further supports the occurrence of high material removal rates because of repeated sliding contact. Additionally, the presence of delamination phenomenon, proven by surface flaking and subsurface crack formation, suggests that the cyclic loading during the wear process induced subsurface stress concentrations that led to initiation and propagation of cracks [40-41].

Figure 8b displays a worn track characterized by shallow, indicating a reduction in abrasive wear severity of the Al6061 reinforced with 1 wt % SiC and 4 wt % CuO joint. The minimal presence of wear debris suggests lower material removal during sliding process, which can be attributed to the increased CuO content. The higher CuO reinforcement likely enhanced the hardness and load-bearing capacity of the composite surface, thereby improving its resistance to micro-cutting and plowing actions, and leading to more stable tribological behaviour under similar sliding conditions [42-43].

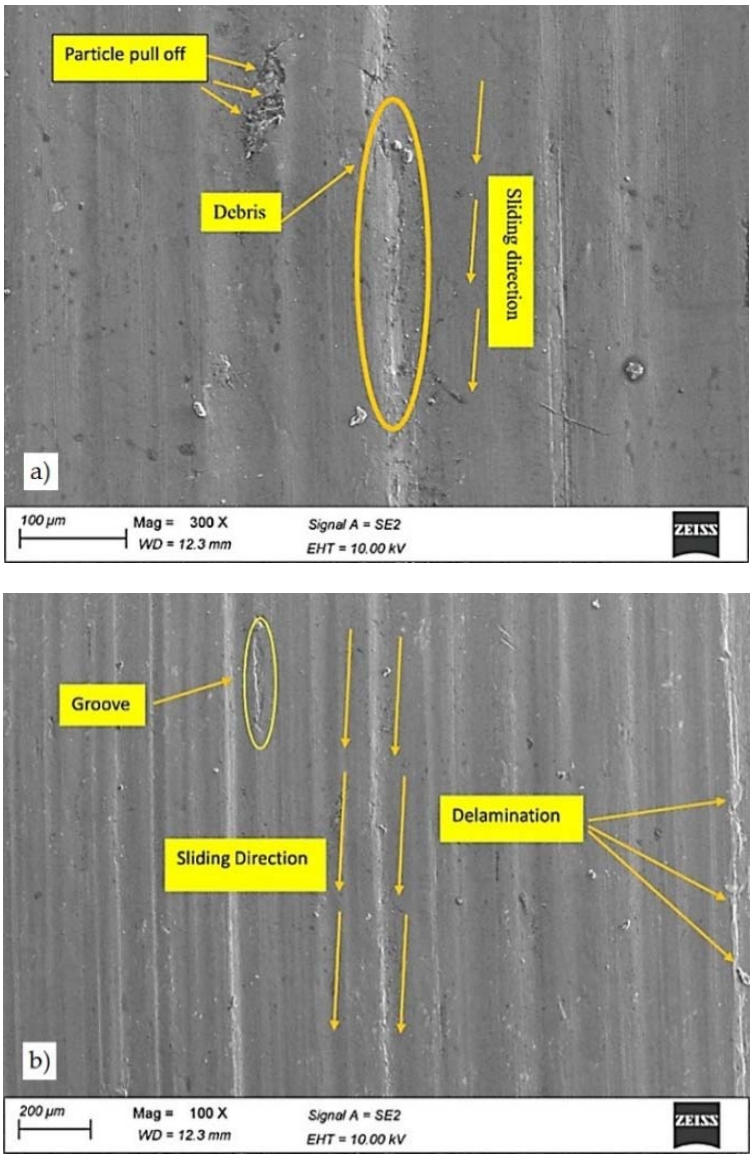

Fig. 8. Worn surface: a) sample 1 with lowest CuO content, b) sample 4 with highest CuO content

4. CONCLUSIONS

- AA6061 plates, having thickness of 6 mm, were reinforced by FSP with a cylindrical taper pin tool and constant process parameters of 1000 rpm rotational speed, and 50 mm/min traverse speed. SiC and CuO particles were incorporated in varying proportions (1 to 4 wt %) to produce surface metal matrix composites and to assess the effects of the reinforcement particles on the mechanical and wear characteristics of the composite material achieved.
- Among all the samples, the sample 3 exhibited the highest mechanical performance, reflected by an optimal combination of strength and ductility. This sample, whose surface was reinforced with 1 wt % SiC and 3 wt % CuO, attained a peak UTS of 190.7 MPa and an elongation of 8.2%, outperforming the other samples reinforced with other particles combinations under the same processing conditions.
- The fractographic analysis of sample 3 surface, made by SEM technique, revealed fewer dimples and no visible cracks, suggesting a more uniform and stable fracture mechanism. The reduced dimple density implies a slight shift toward a less ductile fracture mode, potentially caused by the localized hardening determined by the increased CuO content.
- The highest hardness (75.3 HV) and the Enhanced wear resistance (0.0374 $mm^3/N \cdot m$) were measured in the stir zone of the sample 4 which was reinforced with 1 wt % SiC and 4 wt % CuO by FSP technique, demonstrating the significant influence of larger CuO percentage on the properties of the composite material. The significant increase in hardness is primarily due to the enhanced reinforcement volume fraction, which improves the load-bearing capability and

restricts the dislocation movement through the Orowan strengthening mechanism. The higher amount of CuO, in combination with SiC particles, contributed to better dispersion, increased particle-matrix interface strength, and more effective grain refinement due to the pinning of grain boundaries during the dynamic recrystallization in the stir zone. The worn surface displayed shallow, mild grooves with minimal debris accumulation, indicating reduced abrasive wear and lower material loss during sliding. The results achieved by different testing methods make the optimized FSP-treated AA6061 composite a promising material for industrial applications such as automotive components, aerospace structures, and tooling elements.

REFERENCES

[1] **Md A. P.,** *Fabrication of surface metal matrix composite of AA7075 using friction stir processing,* Journal of Manufacturing Engineering, 2022, vol. 17, iss. 2, pp. 064-067.

[2] **Sriram D., Rao V., Sivasundar V.,** *Microstructure, mechanical properties of dissimilar friction stir welded AA6063/AA5052 alloys, and optimization of process parameters using Box Behnken-TOPSIS approach,* Kovove Materialy - Metallic Materials, 2024, vol. 62, iss. 6., 363.

[3] **Gao J., Wang X., Zhang S., Yu L., Zhang J., Shen Y.,** *Producing of FeCoNiCrAl high-entropy alloy reinforced Al composites via friction stir processing technology,* The International Journal of Advanced Manufacturing Technology, 2020, vol. 110, iss. 1-2, pp. 569-580.

[4] **Yuvaraj N., Aravindan S., Vipin,** *Wear characteristics of Al5083 surface hybrid nano-composites by friction stir processing,* Transactions of the Indian Institute of Metals, 2017, vol. 70, iss. 4, pp. 1111-1129.

[5] **Moustafa E. B., Taha M. A.,** *The Effect of mono and hybrid additives of ceramic particles on the tribological behavior and mechanical characteristics of an Al-based composite matrix produced by friction stir processing,* Nanomaterials, 2023, vol. 13, iss. 14, 2148.

[6] **Behnagh R. A., Besharati Givi M. K., Akbari M.,** *Mechanical Properties, Corrosion Resistance, and Microstructural Changes during Friction Stir Processing of 5083 Aluminum Rolled Plates,* Materials and Manufacturing Processes, 2012, vol. 27, iss. 6, pp. 636-640.

[7] **Ansari M. A., Samanta A., Behnagh R. A., Ding H.,** *An efficient coupled Eulerian-Lagrangian finite element model for friction stir processing,* The International Journal of Advanced Manufacturing Technology, 2019, vol. 101, iss. 5-8, pp. 1495-1508.

[8] **Kumar S., Srivastava A. K., Singh R. K.,** *Fabrication of AA7075 hybrid green metal matrix composites by friction stir processing technique,* Annales de Chimie Science des Matériaux, 2020, vol. 44, iss. 4, pp. 295-300.

[9] **Rao Santha D., Ramanaiah N.,** *Process parameters optimization for producing AA6061/TiB2 composites by friction stir processing,* Strojnícky časopis - Journal of Mechanical Engineering, 2017, vol. 67, iss. 1, pp. 101-118.

[10] **Divekar D., Fuse K., Badheka V.,** *Microstructure and mechanical properties analysis of Al-6061/B4C composites fabricated by conventional and bobbin tool friction stir processing,* The Eurasia Proceedings of Science, Technology, Engineering & Mathematics, 2023, vol. 23, pp. 117-123.

[11] **Kumar M. R., Kaushal A., Ram S. C.,** *Microstructural evolution in composite materials via friction stir processing of Al-6061 cast alloys,* Utilizing Friction Stir Techniques for Composite Hybridization, 2024, pp. 51-78.

[12] **Fatchurrohman N., Farhana N., Marini C. D.,** *Investigation on the effect of friction stir processing parameters on micro-structure and micro-hardness of rice husk ash reinforced Al6061 metal matrix composites,* IOP Conference Series: Materials Science and Engineering, 2018, vol. 319, 012032.

[13] **Rao C. M., Rao K. M.,** *Fabrication and characterization of friction stir processed Al 6061 reinforced with TiB2-Al2O3,* International Journal of Structural Integrity, 2021, vol. 12, iss. 3, pp. 378-387.

[14] **Chanamallu M. R., Saheb K. M.,** *Microstructural and mechanical behavior of Al 6061/SiC-Al2O3 composites processed through friction stir processing,* Metallurgical and Materials Engineering, 2020, vol. 27, iss. 1, pp. 57-73.

[15] **Ouyang J., Yarrapareddy E., Kovacevic R.,** *Microstructural evolution in the friction stir welded 6061 aluminum alloy (T6-temper condition) to copper,* Journal of Materials Processing Technology, 2006, vol. 172, iss. 1, pp. 110-122.

[16] **Shahraki S., Khorasani S., Abdi Behnagh R., Fotouhi Y., Bisadi H.,** *Producing of AA5083/ZrO2 nanocomposite by friction stir processing (FSP),* Metallurgical and Materials Transactions B, 2013, vol. 44, iss. 6, pp. 1546-1553.

[17] **EL-Eraki B. R., EL-Sissi A. R., Khafagi S. M., Nada H. S.,** *Process parameters optimization for producing AA6061/(Al2O3, Gr and Al2O3+Gr) surface composites by friction stir processing,* IOP Conference Series: Materials Science and Engineering, 2019, vol. 610, iss. 1, 012006.

[18] **M. R. Ch., M. R. K.,** *Improving the tribological properties of 6061-T6 Al alloy by surface compositing with nano-size TiB2 ceramic particles via friction stir processing,* International Journal of Engineering and Technology, 2017, vol. 9, iss. 1, pp. 18-23.

[19] **Uday K. N., Rajamurugan G.,** *Analysis of tensile strength on friction stir welded Al 6061 composite reinforced with B4C and Cr2O3 using RSM and ANN,* Engineering Research Express, 2023, vol. 5, iss. 1, 015018.

[20] **Kareem A., Qudeiri J. A., Abdudeen A., Ahammed T., Ziout A.,** *A Review on AA 6061 metal matrix composites produced by stir casting,* Materials, 2021, vol. 14(1), 175.

[21] **Dorward R., Bouvier C.,** *A rationalization of factors affecting strength, ductility and toughness of AA6061-type Al-Mg-Si-(Cu) alloys,* Materials Science and Engineering A, 1998, vol. 254, iss. 1-2, pp. 33-44.

[22] **Alawi O. A., Sidik N. A. C.,** *Mathematical correlations on factors affecting the thermal conductivity and dynamic viscosity of nanorefrigerants,* International Communications in Heat and Mass Transfer, 2014, vol. 58, pp. 125-131.

[23] **Alawi O. A., Mallah A. R., Kazi S., Zubir N. M. N. M., Oon C. S.,** *Thermal Transport Feasibility of (Water + Ethylene Glycol)-Based Nanofluids Containing Metallic Oxides: Mathematical Approach,* IOP Conference Series: Materials Science and Engineering, 2020, vol. 854, iss. 1, 012023.

[24] **Hekmatipour F., M. A. Akhavan-Behabadi, B. Sajadi, M. Fakoor-Pakdaman,** *Mixed convection heat transfer and pressure drop characteristics of the copper oxide-heat transfer oil (CuO-HTO) nanofluid in vertical tube,* Case Studies in Thermal Engineering, 2017, vol. 10, pp. 532-540.

[25] **Ji R., Liu Y., Zhang Y., Cai B., Li X., Zheng C.,** *Effect of machining parameters on surface integrity of silicon carbide ceramic using end electric discharge milling and mechanical grinding hybrid machining,* Journal of Mechanical Science and Technology, 2013, vol. 27, iss. 1, pp. 177-183.

[26] **Nikzad-Dinan M., Jamaati R., Jamshidi Aval H.,** *Enhanced microstructure, strength, and wear resistance of AA2024-AlB2 composites via multi-pass friction stir processing,* J. Mater. Res. Technol., 2015, vol. 36, pp. 4293-4307.

[27] **Sivasundar V., Kakkassery J. J., Jaganathan M., Satheesh Kumar P. S., Vignesh M., Anbuchezhiyan G.,** *ANN modeling and optimization of friction stir welding performance for AA6061 and AA5083 alloy joints,* Proceedings of the Institution of Mechanical Engineers, Part E, 2024.

[28] **Abdeltawab N. M., Elshazly M., Shash A. Y., El-Sherbiny M.,** *Studying the effect of processing parameters on the microstructure, strength, hardness, and corrosion characteristics of friction stir dissimilar welded AA5083 and AA7075 aluminum alloys reinforced with Al-SiC matrix,* Heliyon, 2025, vol. 11, iss. 1, e41362.

[29] **Patil N. A., Pedapati S. R., Marode R. V.,** *Wear Analysis of Friction Stir Processed AA7075-SiC-Graphite Hybrid Surface Composites,* Lubricants, 2022, vol. 10, iss. 10, 267.

[30] **Abdullah M. E., Mohammed M. M., Ahmed F. S., Kubit A., Aghajani Derazkola H.,** *Failure behavior and mechanical*

properties of aluminum alloy-copper nanoparticle surface region fabricated by friction stir processing, Journal of Alloys and Compounds, 2025, vol. 1025, 180343.
[31] **Lakshmaiya N., Vijetha K., Doss A. S. A., Nitesh K. S., Ross N. S., Maranan R.,** *Dual-Scale evaluation of hybrid AL-SIC/Graphene composites: mechanical properties and deep learning-driven machinability insights,* Results in Engineering, 2025, p. 105742.
[32] **Feng W., Baiqing X., Yongan, Z. Yuting Z., Hongwei L., Zhihui L., Xiwu L.,** *Microstructure and mechanical properties of an electron beam welds in a spray-deposited Al-Zn-Mg-Cu alloy,* 13th International Conference on Aluminum Alloys (ICAA 13), 2012, Pittsburgh, Pennsylvania, pp. 921-926.
[33] **Singh T., Tiwari S. K., Shukla D. K.,** *Friction-stir welding of AA6061-T6: The effects of Al2O3 nano-particles addition,* Results in Materials, 2019, vol. 1, 100005.
[34] **Lakshmaiya N., Chukka N. D. K. R., Kaliappan S., Balaji V., Ross N. S., Maranan R.,** *An integrated artificial neural network technique to optimize the various parameters of Pineapple/SiO2/epoxy-based nanocomposites under NaOH treatment,* Results in Engineering, 2025, p. 104737.
[35] **Zhang G. J., Wang R. H., Yuan S. P., Liu G., Scudino S., Sun J., Chen K. H.,** *Influence of constituents on the ductile fracture of Al-Cu-Mg alloys: Modulated by the aging treatment,* Materials Science and Engineering A, 2009, vol. 526, iss. 1-2, pp. 171-176.
[36] **Behtaripour E., Jafarian H. R., Seyedein S. H., Park N., Eivani A. R.,** *High-temperature tensile properties of friction stir processed AA2024 aluminum alloy under varying in situ cooling conditions,* Journal of Materials Research and Technology, 2025, vol. 35, pp. 140-151.
[37] **Pathak A., Mukherjee B., Kant Pandey K., Islam A. et al.,** *Process—structure—property relationship for plasma-sprayed iron-based amorphous/crystalline composite coatings,* International Journal of Minerals Metallurgy and Materials, 2022, vol. 29, iss. 1, pp. 144-152.
[38] **Majumdar J. D.,** *Mechanical and electro-chemical properties of laser surface alloyed AISI 304 stainless steel with WC+Ni+NiCr,* Physics Procedia, 2013, vol. 41, pp. 335-345.
[39] **Feroz Ali L., Soundararajan R., Kovarthanam M., Mohamed Aniq A.,** *Wear and friction properties of AA 7075-T6 with × wt % of WC surface composite fabricated by FSP technique,* Materials Today: Proceedings, 2021, vol. 45, pp. 6482-6487.
[40] **Biswas S., Cenna A., Williams K., Jones M.,** *Subsurface behavior of ductile material by particle impacts and its influence on wear mechanism,* Procedia Engineering, 2014, vol. 90, pp. 160-165.
[41] **Terheci M.,** *Microscopic investigation on the origin of wear by surface fatigue in dry sliding,* Materials Characterization, 2000, vol. 45, iss. 1, pp. 1-15.
[42] **Sabry I., El-Deeb M. S. S., Hewidy A. M., ElWakil M.,** *Mechanical and tribological behaviours of friction stir welding using various strengthening techniques,* Journal of Alloys and Metallurgical Systems, 2024, vol. 7, 100098.
[43] **Lakshmaiya N., Nadh V. S., Kaliappan S., Muthu G., Ross N. S., Maranan R.,** *Enhanced tribological performance of AA6018 aluminium composites reinforced with copper chromate exploring ceramic-based strengthening mechanisms,* Journal of the Australian Ceramic Society, 2025, vol. 61, pp.1871–1878.
[44] **Yunus M., Alfattani R.,** *Assessment of Mechanical and Tribological Behavior of AA6061 Reinforced with B4C and Gr Hybrid Metal Matrix Composites,* Coatings, 2023, vol. 13, iss. 9, p. 1653.
[45] **Kaliappan S. et al.,** *Impact of ALN-SIC nanoparticle reinforcement on the mechanical behavior of AL 6061-Based hybrid composite developed by the Stir Casting Route,* Advances in Materials Science and Engineering, 2022, vol. 2022, pp. 1-8.